MPC-based Path Following Design for Automated Vehicles with Rear Wheel Steering

Chuanyang Yu
Automotive Engineering Group
Technische Universität Ilmenau
Ilmenau, Germany
chuanyang.yu@tu-ilmenau.de

Yanggu Zheng
Dept. of Cognitive Robotics
Delft University of Technology
Delft, The Netherlands
Y.Zheng-2@tudelft.nl

Barys Shyrokau
Dept. of Cognitive Robotics
Delft University of Technology
Delft, The Netherlands
B.Shyrokau@tudelft.nl

Valentin Ivanov*
Automotive Engineering Group
Technische Universität Ilmenau
Ilmenau, Germany
valentin.ivanov@tu-ilmenau.de

***Abstract* — Many studies have been recently exploited to discuss the path following control algorithms for automated vehicles using various control techniques. However, path following algorithm considering the possibility of automated vehicles with rear wheel steering (RWS) is still less investigated. In this study, we implemented nonlinear model predictive control (NMPC) on a passenger vehicle with active RWS for path following. The controller was compared to two other variations of NMPC where the rear steering angle is proportional to the front or fixed to zero. Simulation results suggested that the proposed controller outperforms the other two variations and the baseline controllers (Stanley and LQR) in terms of accuracy and responsiveness.**

Keywords — path following control, model predictive control, automated vehicle, rear wheel steering, simulation

I. Introduction

In recent years, automated driving has attracted considerable attention due to its potential in improving road safety and mobility efficiency. According to Kyriakidis et al. [1], most people believe that fully automated driving could occupy half the market share before 2050. However, there remain ongoing challenges to reach fully automated driving at the moment. Great attention has been paid by to tackle the technical problems therein.

One of these problems is to fulfill the path following task with by developing steering control methods. As summarized in [2] and [3], multiple methods have been developed in the past. Some steering laws (e.g., Stanley and pure pursuit) are derived from the geometric characteristics, whereas other studies adopt control methods including PID, fuzzy control, sliding mode control, linear quadratic regulator (LQR) and model predictive control (MPC).

MPC is considered superior to other aforementioned control methods thanks to its advantage in handling nonlinear dynamic models and constraints [4]. The nonlinear model predictive control (NMPC) was first applied to controlling the steering of automated vehicles by Falcone et al. [5] in the early 2000s. They proposed in [6] to use linear time-variant model to overcome the problem with numerical efficiency and in [7] to further include differential braking for stabilizing the yaw and lateral dynamics when tracking a path for emergency evasion. Li et al. [8] presented an MPC-based trajectory planning and tracking control approach for an automated guided vehicle and managed to achieve trajectory tracking accurately and smoothly. Guo et al. [9] implemented the MPC-based path following controller and proved satisfactory control performance under measurable disturbance. Yoshiba et al. [10] developed MPC-based steering input for lane-change maneuver and conducted desired control performance with the constraint conditions.

Apart from the control methods, various advanced vehicle actuators have been developed and deployed in recent years [11]. Among them, rear-wheel steering (RWS) is closely related to the control of the vehicle's lateral and yaw motion. RWS allows the rear wheels to be steered in order to improve stability at a higher speed and to enhance maneuver ability at a lower speed [12], [13]. The flexibility enabled by RWS in modifying the vehicle's handling characteristics has been considered promising [14]. Hence, RWS is expected to be widely equipped on passenger vehicles with SAE-level 3 and above automated driving system in the future.

In this paper, we propose a novel combination of NMPC and RWS in an attempt to further improve the path tracking performance of automated vehicles. The NMPC formulation is based on [15] whereas the nonlinear bicycle model is extended to incorporate RWS. The prediction model adopts Dugoff model to calculate the lateral tire forces. To demonstrate the advantage of actively controlling the rear wheel angle, three variations of the NMPC were formulated, the first one with no RWS, the second one with a rear steering angle proportional to the front, and the third one with rear steering angle determined in the same way as front steering angle by optimization of NMPC. Meanwhile, we further adopted two baseline controllers from [16], namely the Stanley and LQR controller, to show the superiority of NMPC and RWS.

The rest of the paper is organized as follows. An introduction to vehicle model and tire model is given in section II. Then it is explained in section III about how the controllers are designed. In section IV, various simulations are carried out, and the results are presented and analysed. Finally, conclusions and future directions are pointed out in section V.

II. Vehicle Model

A. Nonlinear Bicycle Model

For sake of reducing the computational load, a nonlinear bicycle model is used for predicting the vehicle's behavior (Fig. 1). The model is not capable of incorporating the lateral load transfer, nor the roll, pitch, or heave dynamics. The

* corresponding author

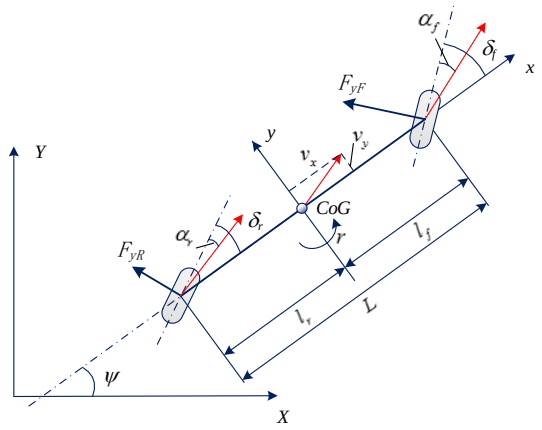

Fig. 1. Bicycle model with RWS, here is an example of parallel steering

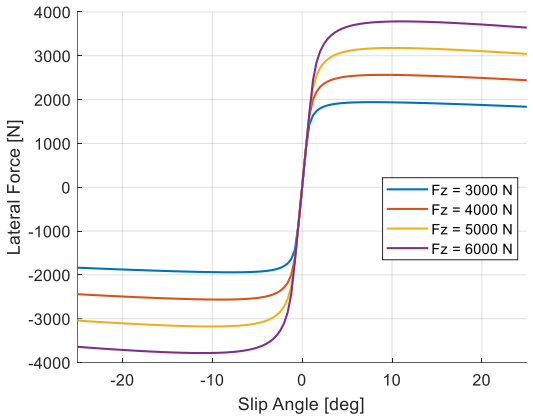

Fig. 2. Tire lateral characteristics

controller handles the path following at constant velocity thus the longitudinal load transfer is also omitted. Hence, the vehicle dynamics are described with the following equations:

$$\begin{aligned} m\left(\dot{v}_x - v_y r\right) &= -F_{yF}\sin\delta_f - F_{yR}\sin\delta_r \\ m\left(\dot{v}_y + v_x r\right) &= F_{yF}\cos\delta_f + F_{yR}\cos\delta_r \\ I_{zz}\dot{r} &= l_f F_{yF}\cos\delta_f - l_r F_{yR}\cos\delta_r \end{aligned} \tag{1}$$

where m denotes the total mass of the vehicle, I_{zz} the yaw moment of inertia of vehicle body around the center of gravity, F_{yF} and F_{yR} denote lateral tire force on the front and rear wheels, respectively. v_x , v_y and r are related to the vehicle's longitudinal, lateral and yaw velocity, respectively. Additionally, l_f and l_r are the distance from the vehicle center of mass to the front axle and rear axle, respectively. δ_f and δ_r denote the road steering angle (RWA) of front wheels and rear wheels, respectively.

According to the geometric relationships in Fig. 1 and by using the small angle approximation, the sideslip angles of the front and rear tires are given by:

$$\begin{aligned} \alpha_f &= \delta_f - \frac{v_y + l_f r}{v_x} \\ \alpha_r &= \delta_r - \frac{v_y - l_r r}{v_x} \end{aligned} \tag{2}$$

where α_f and α_r are the front and rear wheel slip angle, respectively.

The equations above describe the vehicle's motion in the local frame. The local states are then projected to the global frame using (3).

$$\begin{aligned} \dot{X} &= v_x\cos\psi - v_y\sin\psi \\ \dot{Y} &= v_x\sin\psi + v_y\cos\psi \\ \dot{\psi} &= r \end{aligned} \tag{3}$$

Where X and Y are the positions of the vehicle in global coordinate frame, and ψ is heading angle.

B. Tire Model

The Dugoff tire model is used to present the tire nonlinear force characteristics more accurately. The parameters have been tuned to closely match the simulation model. The example lateral forces are shown in Fig. 2. At each time step, the local lateral stiffnesses for front and rear axle, C_f and C_r, are calculated accordingly by means of linearization at the current sideslip angle. The lateral tire forces in the prediction model are then given by:

$$\begin{aligned} F_{yF} &= C_f\alpha_f \\ F_{yR} &= C_r\alpha_r \end{aligned} \tag{4}$$

III. Controller Design

A. System Overview

The structure of the path following controller is shown in Fig. 3. Here, the states of the plant, *x(t)*, are measured by the sensors or calculated by the state estimator, and fed into the controller as initial state of the prediction model at each time step. Meanwhile, parameters related to Dugoff tire model are measured by virtual tire force sensors [17] to calculate the local lateral stiffness, which are updated in the prediction model of NMPC at each time step. The reference of the states *r(t)* contains information about the path to be followed. The optimal control problem (OCP) formulated within the NMPC

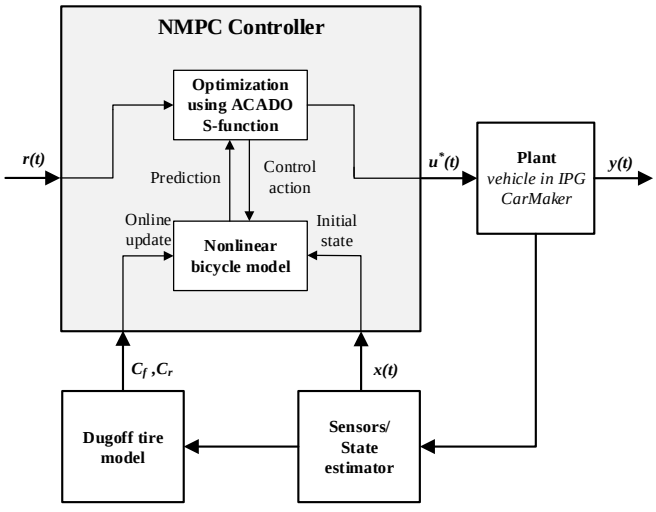

Fig. 3. Structure of NMPC-based path following controller

is solved at each time step using ACADO Toolkit [18] to determine the optimal control input $u^*(t)$, which is eventually transmitted to the steering actuators on the front and rear axle.

B. NMPC Controller Design

The NMPC determines the optimal control input by solving an OCP at each time step. Given the reference output at current time step *k*, a cost function in the form of (5) evaluates whether a control sequence is desirable, based on the model of vehicle dynamics described in Section II. The model predicts the vehicle's behavior through the prediction horizon of *N* steps ahead. Therein, $x(k) = [v_x\ v_y\ r\ X\ Y\ \psi\ \delta_f\ \delta_r]^T$ contains states while $u(k) = [v_{\delta_f}\ v_{\delta_r}]^T$ denotes the control inputs. The last two state variables comes from the fact that, instead of directly commanding the steering angle, we opted for the steering rate as the control input. Therefore, the actual steering angles should be included in the state vector. Such choice allows the controller to generate smooth and feasible command for the steering actuators.

$$J = \sum_{k}^{k+N-1} \left(\left\| r(k) - y(k) \right\|_W^2 + \left\| u^{ref}(k) - u(k) \right\|_Q^2 \right) + \left\| r(k+N) - y(k+N) \right\|_P^2 \tag{5}$$

The cost function mainly penalizes the vehicle's deviation from the reference path with positive definite matrices *W* and *P* for running cost and terminal cost, respectively. The reference state vector $r(k) = [Y^{ref}\ \psi^{ref}\ \delta_f^{ref}\ \delta_r^{ref}]^T$ describes the desired states from reference path, and vector $y(k) = [Y\ \psi\ \delta_f\ \delta_r]^T$ describes the output states. $u^{ref}(k)$ denotes the reference control action and is set $[0\ \ 0]^T$ to penalize the value of control action $u(k)$ through the prediction horizon with weight matrix *Q*. Besides, constraints are set as follows considering the restrictions of the steering dynamics:

$$\begin{aligned} -0.6\ rad &\le \delta_f \le 0.6\ rad \\ -0.5\ rad/s &\le v_{\delta_f} \le 0.5\ rad/s \\ -0.12\ rad &\le \delta_r \le 0.12\ rad \\ -0.1\ rad/s &\le v_{\delta_r} \le 0.1\ rad/s \end{aligned} \tag{6}$$

Thus, an OCP is formulated, which is to minimize cost function (5), subject to (1) to (4) and (6). In this study, the OCP is solved by ACADO Toolkit. To tackle the OCP, ACADO performs various nonlinear programming algorithms [18] at each time step according to the solver-settings. These OCP solving algorithms are exported as C-Code using ACADO Code Generation. The generated C-Code is then compiled to an S-function using MEX-functions of MATLAB. And S-function can be deployed as the control segment into the Simulink model.

Based on this NMPC framework, three variations of the NMPC path following controllers are formulated in this research in order to demonstrate the benefits of actively controlled RWS.

1) NMPC without RWS: In this variation, the rear steering rate is fixed to zero and only the front wheels are turned. The vehicle behaves like a conventional one. This variation enables a fair comparison to the existing path following control methods using only front wheel steering.

2) NMPC with passive RWS: In this case, the rear wheel steering angle is proportional to front wheel steering angle and the ratio is dependent on the vehicle's velocity.

$$\delta_r = p\delta_f = k \frac{-l_f + \dfrac{ml_r}{C_{\alpha_f}(l_f + l_r)} v_x^2}{l_r + \dfrac{ml_f}{C_{\alpha_r}(l_f + l_r)} v_x^2} \delta_f \tag{7}$$

Here, *k* is a tuneable parameter that should be chosen according to the capability of the RWS actuator. Comparing this variation to the one above demonstrates the contribution of RWS to vehicle agility and stability.

3) NMPC with active RWS: In this variant, the rear wheel steering angle is derived in the same way as front wheel steering angle by solving the OCP online. Front wheels and rear wheels of the plant vehicle are steered independently to each other, while the front wheel steering should dominant like conventional passenger cars when making a turn. Comparing this variation to the other two, we can gain some insights into the worthiness of increasing computational complexity.

IV. Simulations

A. Simulation Environment

The controllers are tested in a co-simulation setup between MATLAB/Simulink and IPG CarMaker. IPG CarMaker includes the validated multibody model of vehicle dynamics and Delft-tire model to ensure high fidelity. The parameters of the vehicle, given in Table I, correspond to a mid-size passenger car.

The simulations were first carried out on a laptop PC with Intel® Core™ i7-4700MQ processor and 8GB RAM and later on hard real-time platform dSPACE Scalexio to check real-time feasibility.

B. Simulated Maneuvers

To verify the functionality of the path following controllers, the multiple maneuvers have been considered. In the first scenario, an objective vehicle with a longitudinal speed 60 km/h is driving at a certain distance ahead of the controlled vehicle with a velocity of 80 km/h in the same lane. If no actions are applied, a rear-end collision would happen. Assuming that the adjacent lane is unoccupied, the controlled vehicle could perform an overtake maneuver. An overtake trajectory is planned as follows. Parameterized Sigmoid curves are implemented as overtake reference path to describe

TABLE I. Parameters of Plant Dynamics

Symbol	Introduction		
	Description	***Value***	***Unit***
m	Mass of the vehicle	1644.8	kg
I_{zz}	Body inertia around z-axis	1921.3	kg*m^2
l_f	Distance from front axle to CoG	1.223	m
l_r	Distance from rear axle to CoG	1.527	m
$C_{\alpha f}$	Cornering stiffness of front tires	120000	N/rad
$C_{\alpha r}$	Cornering stiffness of rear tires	190000	N/rad

the relationship between relative longitudinal position and lateral offset as adopted from [19]. One parameterized Sigmoid curve describes a single lane-change maneuver while the entire maneuver consists of two lane-changes. Hence, the complete trajectory consists of two sigmoid curves connected one after another:

$$\begin{cases} y_1(x_1) = \dfrac{w}{1+e^{-\mu x_1}} \\ y_2(x_2) = \dfrac{-w}{1+e^{-\mu x_2}} \end{cases} \text{ with } \begin{cases} x_1 = \Delta x + d_{safe} \\ x_2 = \Delta x - d_{safe} - d_c \end{cases} \tag{8}$$

Where, μ and w are scaling factors in the longitudinal and lateral direction, respectively, and Δx denotes the longitudinal distance between the objective vehicle and ego vehicle regarding Frenet coordinate, d_{safe} is the safety margin for objective vehicle, and d_c is additional overtake distance. The lateral reference of the entire reference path is defined as:

$$Y^{ref} = y_1 + y_2 + y_o \tag{9}$$

Where, y_o is the original lateral offset of both vehicles regarding Frenet coordinate. To determine the exact time of executing overtaking maneuver, the criterion time to collision (*TTC*) is introduced to describe the time before collision:

$$TTC = \frac{\Delta x - l}{v_e - v_o} \tag{10}$$

Where, l is chosen as the typical length of a passenger car, v_e and v_o denote longitudinal velocity of ego vehicle and objective vehicle, respectively. By assuming the objective vehicle's motion is accurately known by the controlled vehicle, Algorithm 1 determines the initiation of the overtake maneuver. Besides the reference lateral position, the reference yaw angle is calculated accordingly to achieve a better path following performance as:

$$\psi^{ref} = \arctan\frac{dY^{ref}}{dx} = \arctan\frac{(Y^{ref}(t) - Y^{ref}(t-T_s))}{(x(t) - x(t-T_s))} \tag{11}$$

In the second simulation scenario, the step lane-change maneuver is carried out with different road conditions to verify the designed controllers in a more critical way.

Algorithm 1: Overtaking algorithm

Input: longitudinal velocity of ego vehicle v_e and objective vehicle v_o, time to collision *TTC*, original lateral offset y_o

Output: lateral reference offset Y^{ref}

```
t ← 4
if v_e − v_o ≤ 0 then
    Y^ref ← y_o
else
    if TTC > t then
        Y^ref ← y_o
    else
        Y^ref ← y_1 + y_2 + y_o
    end if
end if
```

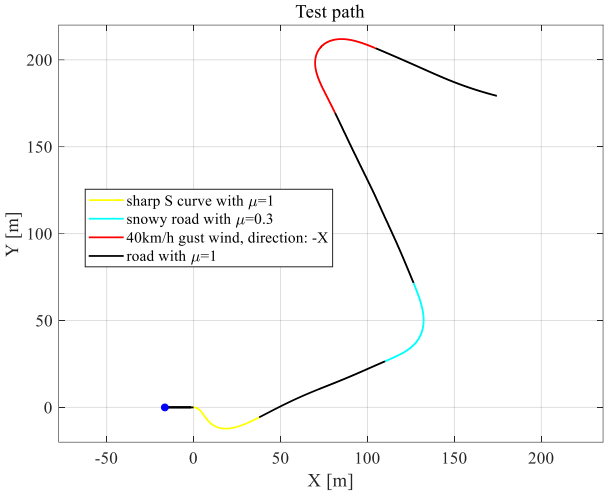

Fig. 4. Road geometry in the simulation scenario

Normally in an automated vehicle system, the reference path should be finely planned by front sequences. In this test scenario, there is a static obstacle ahead of controlled vehicle at the speed of 80 km/h but planning sequence of automated system failed unexpectedly. The step lane-change maneuver may be performed as an evasive maneuver, where a step signal of lateral offset is given to the controller to make the controlled vehicle suddenly change driving lane to avoid collision. Different road friction conditions such as dry asphalt, wet asphalt and asphalt with snow and ice are investigated in the simulation scenario.

In the third test scenario, the three designed controllers and two other path following controllers based on Stanley and LQR respectively from the work [15] are tested to follow the same path, respectively. The test path is defined using a customized road geometry in IPG CarMaker with some additional customized disturbance like gust wind and various road friction as shown in Fig. 4. The reference information of desired path is obtained by road sensor, which generates current lateral and heading deviation between the vehicle and the preview point on the desired path regarding Frenet coordinate. The preview distance is set to 3 meters, and longitudinal speed is set to 30 km/h.

C. Simulation Results

The first simulation scenario is visualized in Fig. 5(a), which affirms that the overtaking trajectory and the moment of initiation are properly chosen. The front and rear steering angles are given in Fig. 5(b) and Fig. 5(c), respectively.

As a result, it is intuitive to recognize the steering pattern of two adjacent lane-change maneuvers. In Fig. 5(d) we can observe a higher tracking accuracy achieved by combining NMPC with active RWS, compared to the passive- and non-RWS variations.

The simulation results from the step lane-change scenario are presented in Fig. 6. The criteria including overshoot, rise time and settling (within 2% range) time are adopted to evaluate performance of the controllers.

The results presented in Table II demonstrate that the proposed variations with RWS yield quicker response in all friction conditions compared to the variation without RWS, despite the higher but still acceptable overshoot especially in

(a) Visualization of overtaking maneuver

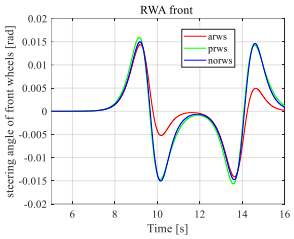

(b) Front wheel steering angle

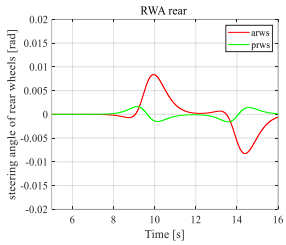

(c) Rear wheel steering angle

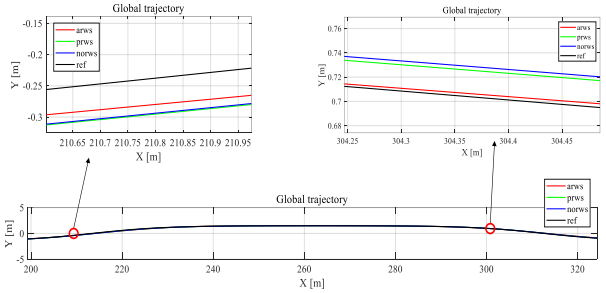

(d) Global position of overall overtaking maneuver

Fig. 5. Simulation results of overtaking maneuver

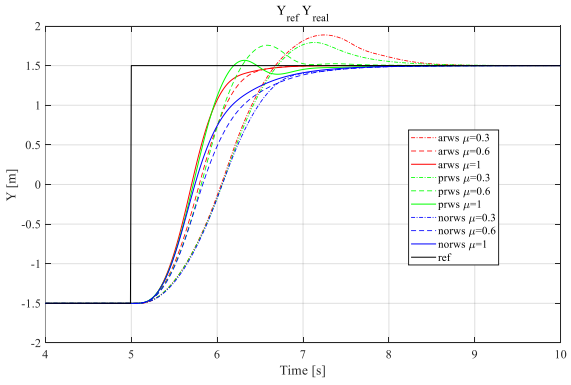

(a) Difference of lateral offset

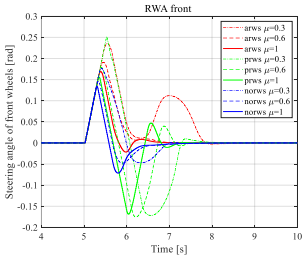

(b) Front wheel steering angle

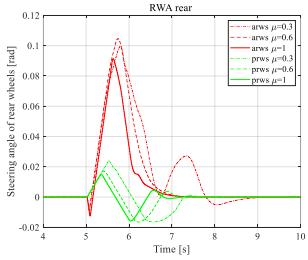

(c) Rear wheel steering angle

Fig. 6. Simulation results of step lane-change

TABLE II. RESULTS OF SIMULATION: STEP LANE-CHANGE

Test case	Criteria			
	Overshoot (m)	***Overshoot (%)***	***Rise time(s)***	***Settling time(s)***
arws_μ=0.3	0.39	13.00	1.50	3.21
arws_μ=0.6	0	0	1.21	1.49
arws_μ=1	0	0	1.07	1.47
prws_μ=0.3	0.29	9.67	1.51	2.94
prws_μ=0.6	0.26	8.67	1.15	1.91
prws_μ=1	0.07	2.33	1.03	1.94
norws_μ=0.3	0	0	1.63	2.32
norws_μ=0.6	0	0	1.56	2.31
norws_μ=1	0	0	1.43	2.19

the low-friction case. It implies that, in the case of an evasive maneuver, RWS may improve the agility of the vehicle with a little risk of exceeding the road boundary. Compromising among all the criteria, the proposed controller, NMPC with active RWS, has the best control performance in the medium- and high-friction cases.

The simulation results of the third scenario, where the vehicle drives on an arbitrary path, are shown as Fig. 7. All tested controllers are able to follow the designated path without exceeding the road boundary. The criteria reflecting the tracking accuracy, including the max, mean and standard deviation (SD) of the lateral and heading error, are summarized in Table III.

In terms of lateral position, the proposed controller yields the smallest error among all the controllers. The other two

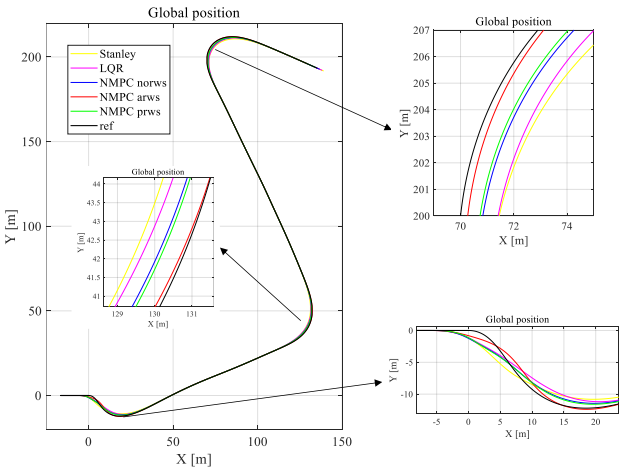

(a) Difference of global position

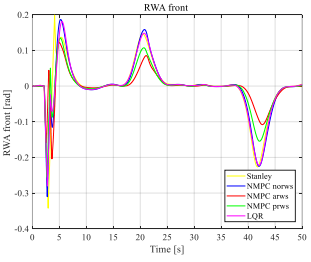

(b) Front wheel steering angle

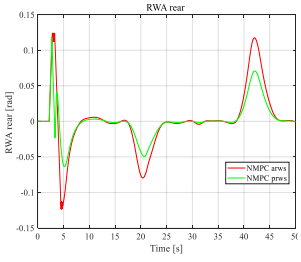

(c) Rear wheel steering angle

Fig. 7. Simulation results of benchmark

TABLE III. RESULTS OF SIMULATION: BENCHMARK

Criteria	Considered controllers				
	Stanley	*LQR*	*NMPC*		
			without RWS	*passive RWS*	*active RWS*
Max lateral error, m	1.74	1.58	1.53	1.58	1.04
Mean lateral error, m	0.31	0.24	0.15	0.15	0.07
SD of lateral error	0.46	0.40	0.26	0.25	0.16
Max heading error, rad	0.64	0.64	0.62	0.57	0.62
Mean heading error, rad	0.10	0.11	0.11	0.10	0.08
SD of heading error	0.15	0.17	0.17	0.15	0.15

variations of NMPC also outperform LQR and Stanley significantly despite the absence of actively controlled RWS. The controllers show similar performance of heading angle tracking, with the proposed solution of combining NMPC with active RWS marginally standing out in terms of the mean error.

V. CONCLUSION

In this study, we developed an NMPC-based path following control method for automated vehicles with the inclusion of actively controlled RWS. The controller updates the tire parameters in a Dugoff model using the measurements of virtual tire force sensors. In addition, we formulated under the same framework two other variations of NMPC controller with passive and no RWS. The performance of proposed controllers has been tested in various simulation scenarios and compared to baseline controllers including Stanley and LQR. The simulation results suggest that the proposed solution has the best overall path following performance. The advantage of the proposed solution over the variations with limited or no RWS functionality demonstrates the benefit of actively controlled RWS. Meanwhile, the performance gain over Stanley and LQR controllers indicates the strength of the NMPC framework. Nevertheless, this paper only focuses on controlling the steering of the vehicle. The longitudinal dynamics are temporarily neglected, excluding the possibility of taking sharp corners with a lower speed and not utilizing the differential driving / braking for generating yaw moments. The comprehensive use of longitudinal and lateral actuators for path following will be investigated in the future works, where the objective of the control may further include safety- and comfort-related concerns.

REFERENCES

[1] Kyriakidis, M., Happee, R., & de Winter, J. C. (2015). Public opinion on automated driving: Results of an international questionnaire among 5000 respondents. *Transportation research part F: Traffic Psychology and Behaviour*, 32, 127-140.

[2] Sorniotti, A., Barber, P., and De Pinto, S. (2017). "Path Tracking for Automated Driving: A Tutorial on Control System Formulations and Ongoing Research," *Automated Driving*, Springer International Publishing, 71–140. .

[3] Rupp, A., and Stolz, M. (2017). "Survey on Control Schemes for Automated Driving on Highways," *Automated Driving*, Springer International Publishing, 43–69.

[4] Garcia, C. E., Prett, D. M., & Morari, M. (1989). Model predictive control: theory and practice—a survey. *Automatica*, 25(3), 335-348.

[5] Borrelli, F., Falcone, P., Keviczky, T., Asgari, J., & Hrovat, D. (2005). MPC-based approach to active steering for autonomous vehicle systems. *Int. Journal of Vehicle Autonomous Systems*, 3(2-4), 265-291.

[6] Falcone, P., Borrelli, F., Asgari, J., Tseng, H. E., & Hrovat, D. (2007). Predictive active steering control for autonomous vehicle systems. *IEEE Transactions on Control Systems Technology*, 15(3), 566-580.

[7] Falcone, P., Eric Tseng, H., Borrelli, F., Asgari, J., & Hrovat, D. (2008). MPC-based yaw and lateral stabilisation via active front steering and braking. *Vehicle System Dynamics* , 46(S1), 611-628.

[8] Li, J., Ran, M., Wang, H., & Xie, L. (2019). MPC-based Unified Trajectory Planning and Tracking Control Approach for Automated Guided Vehicles. *IEEE 15th International Conference on Control and Automation*, 374-380.

[9] Guo, H., Cao, D., Chen, H., Sun, Z., & Hu, Y. (2019). Model predictive path following control for autonomous cars considering a measurable disturbance: Implementation, testing, and verification. *Mechanical Systems and Signal Processing*, 118, 41-60.

[10] Yoshida, H., Shinohara, S., & Nagai, M. (2008). Lane change steering manoeuvre using model predictive control theory. Vehicle System Dynamics, 46(S1), 669-681.

[11] Shyrokau, B., Wang, D., Savitski, D., Hoepping, K., & Ivanov, V. (2015). Vehicle motion control with subsystem prioritization. Mechatronics, 30, 297-315.

[12] Ma, F., Shen, Y., Nie, J., Li, X., Yang, Y., Wang, J., & Wu, G. (2020). Trajectory Planning and Tracking for Four-Wheel-Steering Autonomous Vehicle with V2V Communication. *SAE Technical Paper*, No. 2020-01-0114.

[13] Beal, C. E., & Gerdes, J. C. (2010). Predictive control of vehicle roll dynamics with rear wheel steering. *American Control Conference*, 1489-1494.

[14] Yu, S., Wang, J., Wang, Y., & Chen, H. (2016). Disturbance observer based control for four wheel steering vehicles with model reference. *IEEE/CAA Journal of Automatica Sinica*, *5*(6), 1121-1127.

[15] N. Chowdhri, L. Ferranti, F. Santafe Iribarren, B. Shyrokau (2020). Integrated Nonlinear Model Predictive Control for Automated Driving, *Control Engineering Practice*, 106, 104654.

[16] Lu, Z., Shyrokau, B., Boulkroune, B., Van Aalst, S., & Happee, R. (2018). Performance benchmark of state-of-the-art lateral path-following controllers. *IEEE 15th International Workshop on Advanced Motion Control*, 541-546.

[17] Iyer, K., Shyrokau, B., Ivanov, V. (2020) Offline and Online Tyre Model Reconstruction by Locally Weighted Projection Regression. *IEEE International Workshop on Advanced Motion Control*, Kristiansand, Norway.

[18] Houska, B., Ferreau, H. J., & Diehl, M. (2011). ACADO toolkit−An open ‐ source framework for automatic control and dynamic optimization. *Optimal Control Applications and Methods*, 32(3), 298-312.

[19] Huang, X., Zhang, W., & Li, P. (2019). A Path Planning Method for Vehicle Overtaking Maneuver Using Sigmoid Functions. *IFAC-PapersOnLine*, 52(8), 422-427.